Available online at www.sciencedirect.com
SCIENCE DIRECT®
Nuclear Engineering and Design 236 (2006) 115–127
Nuclear Engineering and Design
www.elsevier.com/locate/nucengdes

Effect of specimen sizes, specimen shapes, and placement directions on compressive strength of concrete

Seong-Tae Yi [a,*], Eun-Ik Yang [b], Joong-Cheol Choi [c]

[a] *Department of Civil Engineering, Chung Cheong University, 330 Wolgok-ri, Kangnae-myun, Cheongwon-kun, Chungbuk-do 363-792, South Korea*
[b] *Department of Civil Engineering, Kangnung National University, 123 Chibyon-dong, Gangneung-si, Kangwon-do 210-702, South Korea*
[c] *Department of Structure, Dongsung Engineering Co., Ltd., 15-2 Suckchon-dong, Songpa-gu, Seoul-si 138-842, South Korea*

Received 28 January 2005; received in revised form 28 July 2005; accepted 4 August 2005

Abstract

The compressive strength of concrete is used as the most basic and important material property when reinforced concrete structures are designed. It has become a problem to use this value, however, because the control specimen sizes and shapes may be different from country to country.

In this study, the effect of specimen sizes, specimen shapes, and placement directions on compressive strength of concrete specimens was experimentally investigated based on fracture mechanics. Experiments for the Mode I failure were carried out by using cylinder, cube, and prism specimens. The test results are curve-fitted using least square method (LSM) to obtain the new parameters for the modified size effect law (MSEL). The analysis results show that the effect of specimen sizes, specimen shapes, and placement directions on ultimate strength is present. In addition, correlations between compressive strengths with size, shape, and placement direction of the specimen are investigated.

1. Introduction

All materials have specific inherent material properties. For each material, the properties are considered unique when they are independent of a specimen size and shape. For design purposes, the concrete compressive strength of standard cylinder (Ø150 mm × 300 mm) is accepted as the most basic and important material property. However, the common notion that concrete compressive strength is a unique material property is an erroneous one since the compressive strength of concrete changes based on specimen sizes and shapes due to its fracture characteristics.

For most countries, sizes and shapes of test specimens to determine the compressive strength of the concrete are different. However, commonly used specimens are cylinders and cubes. Cylinders

* Corresponding author. Tel.: +82 43 230 2315; fax: +82 43 230 2319.
E-mail address: yist@ok.ac.kr (S.-T. Yi).

0029-5493/$ – see front matter © 2005 Elsevier B.V. All rights reserved.
doi:10.1016/j.nucengdes.2005.08.004

Nomenclature

B	empirical constant
CF	conversion factor
cy, cu, pr	shape of the specimens (i.e., cylinders, cubes, and prisms, where the placement direction of cubes and prisms are normal to the loading direction)
cu,p, pr,p	specimens' shape when the placement direction of specimens is parallel to the loading direction
d	characteristic dimension, diameter of cylinders, the smallest size of cubes and prisms
d_a	maximum aggregate size
DCB	double cantilever beam
f'_c	compressive strength of standard concrete cylinders
$f_{cu}(d)$	compressive strength with size of cubes
$f_{cu,p}(d)/f_{pr,p}(d)$	compressive strengths with size of cubes and prisms when the placement direction is parallel to the loading direction
$f_{cy}(d)$	compressive strengths of general cylinders
$f_{pr}(d)$	compressive strength with size of prisms
FPZ	fracture process zone
f'_t	direct tensile strength
f_u	ultimate axial stress
h	height of cylinder specimen
HSC	high-strength concrete
l_o	width of crack band ($=\lambda_o d_a$)
MSEL	modified size effect law
NSC	normal-strength concrete
R^2	correlation coefficient
s/a	fine aggregate/(fine aggregate + coarse aggregate)
SEL	size effect law
w/c	water-cementitious materials ratio of the concrete

Greek symbols

α	empirical constant
λ_o	approximate constant (=2.0)
σ_o	size independent stress ($=\alpha f'_t$)
$\sigma_N(d)$	nominal strength at failure

(Ø150 mm × 300 mm) are used in the United States, South Korea, France, Canada, Australia, and other countries whereas cubes (150 mm) are the standard specimens used in the United Kingdom, Germany, and many other European countries. There are several countries (i.e., Norway uses Ø150 mm × 300 mm cylinder and 150 mm cube), where tests are made on both cylinders and cubes.

Due to the differences in the shape, height/diameter ratio, and end restraint occurred by the machine platen, cylinder and cube strengths obtained from the same batch of concrete could differ. Namely, it is noted that cubes have higher strength than cylinders. Since the early 1900s, many studies (Gonnerman, 1925; Gyengo, 1938; Murdock and Kesler, 1957) on this field have been carried out. Most researches were focused on some guidelines for translating the compressive strength of concrete determined from nonstandard specimens to that of standard specimens' strength and relationships between cylinder strength and cube strength for normal-strength concrete (NSC). Generally, a factor of 1.2 is used to convert cylinder strength to cube strength for NSC. For cubes, however, the factor is gradually decreased from the value of 1.2 as the concrete strength increases. Namely, for high-strength concrete (HSC), the influence of specimen shape is decreased. CEB-FIP Model Code 1990 (1993) also indicates that the ratio of the cube strength to cylinder strength with increasing compressive strength of concrete decreases progressively from 1.25 to 1.12. Above-mentioned 1.25 and 1.12 are the ratios corresponding to the cylinder compressive strengths of 40 and 80 MPa, respectively.

Murdock and Kesler (1957) found that the correction factor depends on the level of concrete strength and that HSC is less affected than LSC. This factor is important to set up a bridge between the analytical or design approaches for structural concrete developed based on the cylinder or/and cube strengths. For the whole range of concrete grades currently in use, however, systematic studies on this topic are scarce. Recently, Mansur and Islam (2002) evaluated the interpretation of concrete strength for nonstandard specimens. However, their studies were limited to interpret strengths between cylinders and cubes.

Typical compression members generally used for design and construction of concrete structures are columns. If the cover of the column is removed, the

interior shape of columns reinforced with spirals and stirrups will be similar to a cylinder and a prism, respectively. Where most columns have a square or rectangular cross-section reinforced with stirrups. In column designs, the cover is not considered as the structural member. In this study, the prism specimen was adopted to investigate actual characteristics of the column reinforced with stirrups.

The purpose of this study is to experimentally investigate the characteristics of axial compressive failure of the concrete and suggest the equations for the prediction of compressive strengths with specimen size, specimen shape, and placement direction based on the fracture mechanics. In addition, a mutual relationship between these equations was also evaluated. Finally, to obtain the concrete compressive strength of cylindrical specimen shape from other specimen shapes, model equations commonly applicable to both specimen shapes (i.e. (1) cylinders and cubes and (2) cylinders and prisms) are suggested. It could be of considerable help to designers and contractors should translate the concrete compressive strength of cubes or prisms to the strength of standard cylinders. This study only deals with axial compressive failure between two representative compressive failure modes of axial compression and flexural compression.

2. Application of MSEL on concrete compressive failure

Based on the size effect law (SEL) derived by Bazant (1984), Kim and Eo (1990) proposed the modified size effect law (MSEL, Eq. (1)) by adding the size independent strength $\sigma_o(=\alpha f_t')$ to SEL that can predict the strength of concrete members with or without initial cracks and with similar or dissimilar cracks. This concept is also proposed by Bazant (1987, 1993) and Bazant and Xiang (1997) with a different approach.

$$\sigma_N(d) = \frac{Bf_t'}{\sqrt{1 + d/\lambda_o d_a}} + \alpha f_t' \quad (1)$$

where $\sigma_N(d)$ is the nominal strength; f_t' the direct tensile strength; d the characteristic dimension; d_a the maximum aggregate size; and B, λ_o, and α are the empirical constants.

Although the failure mechanism and size effect of tensile failure have been studied extensively, the behavior of compressive failure has not been sufficiently studied in comparison to the tensile failure mechanism. Concrete is a construction material normally used to withstand compressive force. Accordingly, the study on this field is necessary. Since it is logical to extend the tensile size effect research to compressive failure research, the direct tensile strength f_t' used in MSEL must be substituted by the compressive strength of standard cylinder f_c' in the new model equation for the prediction of compression loaded size effect. This substitution can be done because even though the failure mechanism of tensile failure is different than compressive failure, the ultimate failure of both specimens is due to the propagation of macro-crack indicating a localized tension or Mode I failures. Therefore, it is safe to assume that the tensile fracture-based concept can be applied to compressive failure as well. The validity of MSEL was demonstrated by regression analyses on available test data for splitting tensile strength, shear strength, and uniaxial compressive strength (1990).

As an application of MSEL, some researches (Kim et al., 1999, 2000, 2001, 2004, 2005; Yi et al., 2002) have been performed on unnotched and notched cylindrical specimens subjected to uniaxial compressive force, axially loaded double cantilever beam (DCB), and C-shaped specimens subjected to flexural compression force. In Eq. (1), the width of crack band l_o is empirically found to be related to the maximum aggregate size d_a (in this study, $d_a = 13$ mm), e.g., $l_o = \lambda_o d_a$ in which λ_o is an approximate constant with values between of 2.0 and 3.0 (Bazant, 1984; Kim et al., 1999, 2000, 2001). In the regression analysis, this constant is selected as 2.0 where $l_o = 2.0 d_a = 26.0$ mm.

In the previous study (Kim et al., 1999), Eq. (2) was proposed to obtain the compressive strength of cylindrical concrete specimens with various diameters and height/diameter ratios. For this purpose, the effects of the maximum aggregate size on the fracture process zone (FPZ) were considered and the concept of characteristic length was newly introduced. In the study, numbers of specimens with $h/d = 2.0$ and $h/d \neq 2.0$ are 222 and 456, respectively. The method to determine the characteristic length is derived and explained by Kim and Eo (1990):

$$\sigma_N(h, d) = \frac{0.4 f_c'}{\sqrt{1 + (h - d)/5}} + 0.8 f_c' \quad (2)$$

where height of cylinder specimen h and diameter of cylinder specimen d are in cm. Eq. (2) was compared to the ASTM standard (ASTM C 42) (1999) and it is noted that the prediction values of Eq. (2) are less than those of the ASTM standard, but the difference is minimal.

3. Test specimens and experimental procedure

In this study, the effect of specimen sizes, specimen shapes, and placement directions on concrete compressive strengths for various strength levels widely used is evaluated. Namely, after confirming independently the size effect of cylinders, cubes, and prisms, correlations between compressive strengths with size, shape, and placement direction of the specimen are investigated. In addition, the effect of placement direction and strength level, respectively, on size effect and shape effect is also clarified.

3.1. Mixture proportioning

The concrete mixture proportions selected are listed in Table 1. Type I Portland cement is used in all mixtures. Crushed gravel is used as the coarse aggregate and the maximum aggregate size is 13 mm. In addition, a high-range water-reducing admixture and vibration table is used to improve workability and consolidation of concrete. Cylinders are cast vertically and cubes and prisms are cast vertically and horizontally, on a level surface. Specimens were prepared in steel moulds on a vibration table (60 Hz, 0.4 mm) with a maximum vibration time of 10 s. After casting, all specimens were subjected to moist-curing. The cylinders were demoulded at 24 h of age. After removal of the mould they were stored in a standard moist room at a temperature of $20 \pm 3\,^{\circ}C$ until the moment of test. The expected average concrete compressive strengths at 28 days were 20, 40, 60, and 80 MPa, correspondingly.

Table 2
Shape and dimension of specimens

Shape	Dimension (mm)
Cylinder (cy)	$\phi 50 \times 100$, $\phi 100 \times 200$, $\phi 150 \times 300$, $\phi 200 \times 400$
Cube (cu, cu,p)	$50 \times 50 \times 50$, $100 \times 100 \times 100$, $150 \times 150 \times 150$, $200 \times 200 \times 200$
Prism (pr, pr,p)	$50 \times 50 \times 100$, $100 \times 100 \times 200$, $150 \times 150 \times 300$, $200 \times 200 \times 400$

3.2. Details of test specimens

The dimensions and shapes used in the experiments are shown in Table 2. In the case of smaller specimen size, more specimens are tested since more data scattering is expected. In Tables 2 and 3, the nomenclatures cy, cu, and pr represent the shape of the specimens (i.e., cylinders, cubes, and prisms, where the placement direction of cubes and prisms are normal to the loading direction). In addition, cu,p and pr,p also represent the specimens' shape when the placement direction of specimens is parallel to the loading direction. These nomenclatures are used in suggesting Eqs. (3)–(7).

3.3. Test procedure

The axial compressive load is applied using universal testing machines (UTM, closed-loop servo-hydraulic testing machine) with a capacity of 1000, 2500, and 7500 kN using a displacement control method. The experiment was performed using a displacement control method of 0.003 mm/s velocity. The rate was applied continuously and without shock. Loads were measured continuously using load cells until the specimen failed.

Table 1
Mixture proportions of concrete

w/c (%)	s/a (%)	Unit weight (kg/m^3)					Super plasticizer[a] (%)	f'_c (MPa)
		Water	Cement	Sand	Gravel[b]	Silica fume		
67	50	185	276	900	962	–	–	27.0
50	48	180	360	837	970	–	–	42.9
35	46	175	500	755	948	–	1.0	65.9
28	44	165	531	692	942	59	2.5	78.1

[a] Super plasticizer (high-range water-reducing admixture), ratio of cement weight.
[b] Maximum aggregate size of 13 mm.

4. Experimental results and evaluation

4.1. Experimental results

Table 3 tabulates the experimental data of ultimate stress f_u with specimen size d, specimen shape, and placement direction. The experimental data of compressive strength f'_c are also shown. They are the averaged results from three identical Ø150 mm × 300 mm cylinders in the series. Where f'_c is the maximum stress, usually considered as the compressive strength of concrete and determined in accordance with ASTM C 39 (2001). In Table 3, "–" means that due to operating problems of data acquisition system it was impossible to obtain f_u.

HSC shows more brittle behavior than NSC. This means that the size of FPZ and the size effect of HSC, respectively, are smaller and more apparent than NSC. This will be also considered in Section 4.5.1.1.

4.2. Size effect for cylinders

Eq. (3) was obtained from the least square method (LSM) regression analyses (Benjamin and Cornell, 1970; IMSL Library) for cylinders.

$$f_{cy}(d) = \frac{0.49 f'_c}{\sqrt{1 + d/2.6}} + 0.81 f'_c \quad (3)$$

where compressive strength of general cylinder $f_{cy}(d)$ and compressive strength of standard cylinder f'_c are in MPa and diameter d is in cm. The term "general" represents the cylinders with arbitrary chosen dimensions. Fig. 2 shows the value $f_{cy}(d)/f'_c$ as a function of the diameter d. In this study, we conclude that the strength ratio approaches a limit with an increasing diameter d. In this figure, the solid rectangular data points and the thick solid line represent, respectively, experimental data of this study and the results from Eq. (3). The correlation coefficient (R^2) of Eq. (3) with experimental data is 0.98 and the comparison indicates that the proposed equation gives a good prediction.

The results from Eq. (2) are also given in Fig. 1 as a dashed line. When Eq. (3) is compared with Eq. (2), it can be seen that compressive strengths of specimens with a diameter greater than 50 mm show similar values as shown in Fig. 1. However, when the diameter is approximately 50 mm or less than 50 mm, the results are slightly different since maximum aggre-

Table 3
Ultimate axial stresses f_u and compressive strengths f'_c obtained from this experiment with w/c, specimen size, specimen type, and placement direction (unit of specimen sizes; mm)

f_u (MPa)																						f'_c (MPa)	w/c (%)
Cylinder					Cube						Prism												
cy (50)	cy (50)	cy (100)	cy (150)	cy (200)	cu (50)	cu (50)	cu (100)	cu (150)	cu (200)	cu,p (50)	cu,p (50)	cu,p (100)	cu,p (150)	cu,p (200)	pr (50)	pr (50)	pr (100)	pr (150)	pr (200)	pr,p (50)	pr,p (50)	pr,p (100)	pr,p (150)	pr,p (200)		
28.5	27.4	28.2	26.8	25.3	35.2	36.4	30.9	33.3	31.8	43.8	39.6	37.0	33.6	33.2	33.3	33.2	27.2	27.1	24.8	32.5	34.0	26.8	25.6	26.1	27.0	67
27.8	27.1	27.6	27.2	24.3	32.6	37.5	32.0	33.9	29.7	39.6	40.5	34.7	35.0	32.8	29.8	33.9	28.4	26.4	26.5	31.1	32.5	26.1	25.6	26.1		
29.2	29.1	28.1	27.1		38.5	37.0	33.8	33.2		39.1	37.3	36.3	32.1		30.4	34.3	30.1	26.9		30.2	29.3	27.3	25.3			
		26.5					32.1					34.5					29.2					27.1				
50.4	45.8	48.1	44.2	43.7	61.7	62.1	51.0	45.7	46.2	66.4	66.3	52.0	43.4	50.5	51.5	53.5	44.7	37.0	43.5	50.7	53.2	45.6	37.2	44.3	42.9	50
52.5	43.1	45.5	40.4	46.5	63.1	58.1	49.6	44.3	–	67.4	66.9	50.5	46.9	49.6	48.0	46.6	41.0	34.8	43.6	48.2	48.5	41.6	35.4	45.0		
44.2	47.2	43.9	44.2		61.6	64.9	44.8	43.7		71.6	65.4	51.7	48.7		47.9	49.3	43.6	39.3		51.2	51.5	41.0	37.0			
		45.2					52.6					51.3					42.4					41.4				
69.4	74.8	67.5	62.7	64.4	82.2	82.1	73.5	65.7	66.8	94.9	94.3	73.3	74.0	75.0	68.8	64.2	66.7	51.0	50.4	69.9	76.7	63.0	60.6	64.8	65.9	35
71.1	72.9	66.6	66.3	66.5	77.0	–	74.8	70.4	64.8	83.5	90.8	74.4	71.1	72.3	68.9	65.0	68.6	53.5	59.2	68.1	70.4	64.4	63.5	59.8		
74.0	74.9	65.5	68.8		79.8	–	71.1	–		88.5	94.4	74.1	–		71.7	66.9	59.6	62.6		72.0	69.8	63.8	–			
		64.4					–					74.9					59.7					65.6				
97.8	92.4	75.9	80.1	71.3	95.0	95.7	81.2	75.8	57.0	102	110	86.0	91.6	72.1	81.8	86.9	74.3	56.5	60.2	92.1	90.2	73.6	83.3	65.1	78.1	28
91.5	83.4	79.9	76.1	–	100.	89.6	80.5	–	–	99.7	102	86.1	80.3	67.8	90.8	72.2	68.1	68.8	59.1	86.7	92.9	69.6	79.0	66.5		
92.5	–	80.6	–		90.2	94.1	84.2	–		100	101	–	79.4		85.5	91.2	71.3	73.8		84.7	94.1	71.6	79.5			
		84.0					–					–					67.3					68.4				

Note. "–" means that due to operating problems of data acquisition system it was impossible to obtain f_u.

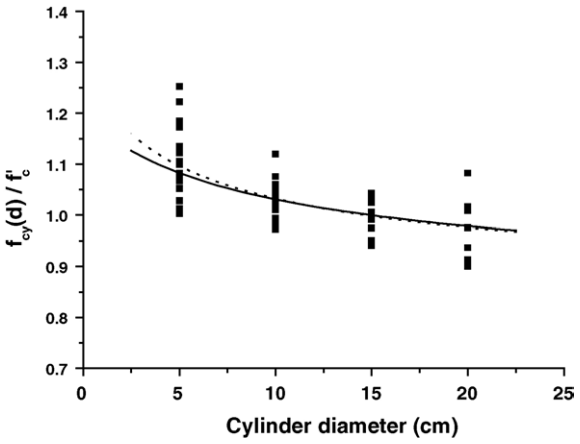

Fig. 1. Size effect for cylinders.

gate size is different. More specifically, Eq. (2) is obtained from tests with maximum aggregate size of approximately 25.0 mm. Even though Eq. (2) has been derived from the test results of $d_a \approx 25.0$ mm, according to the published paper by Kim et al. (1999) in ACI, Eq. (2) is independent of d_a and therefore it can be used for any aggregate size. Therefore, the aggregate size of 13.0 mm can be compared for this study.

4.3. Size effect for cubes

Eq. (4) is obtained from the regression analyses for cubes and the results are graphed and shown in Fig. 2. This figure shows the value $f_{cu}(d)/f'_c$ as a function of the specimen size d and the strong size effect for compressive strengths of cubes. The correlation coefficient of Eq. (4) is 0.94.

$$f_{cu}(d) = \frac{1.17 f'_c}{\sqrt{1 + d/2.6}} + 0.62 f'_c \quad (4)$$

where compressive strength with size of cubes $f_{cu}(d)$ and compressive strength f'_c are in MPa and size of the cube d is in cm.

4.4. Size effect for prisms

Eq. (5) is obtained from the analyses for prisms and the results are graphed and shown in Fig. 3. This figure shows the value $f_{pr}(d)/f'_c$ as a function of the specimen size d. The correlation coefficient of Eq. (5) is 0.95. Eq. (5) shows a good agreement with the experimental results.

$$f_{pr}(d) = \frac{1.02 f'_c}{\sqrt{1 + d/2.6}} + 0.52 f'_c \quad (5)$$

where compressive strength with size of prisms $f_{pr}(d)$ and compressive strength f'_c are in MPa and the smallest size of the prism d is in cm.

By comparing Eqs. (3)–(5), it can be seen that the α values of the MSEL are the largest in Eq. (3) and decreasing accordingly. This is because, for cubes, the stress is concentrated on the edge of the specimen. In addition, for prisms, it is not only due to the stress concentration phenomenon but also because as it is

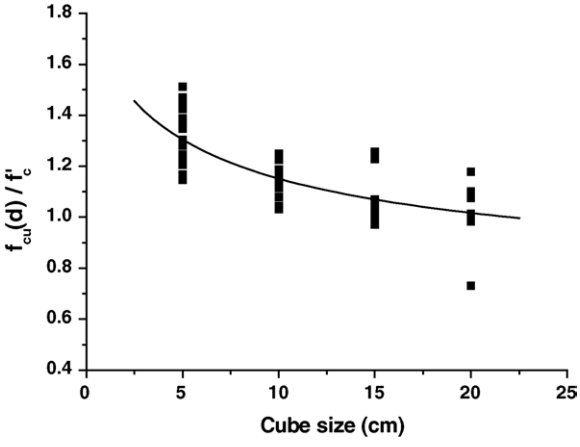

Fig. 2. Size effect for cubes.

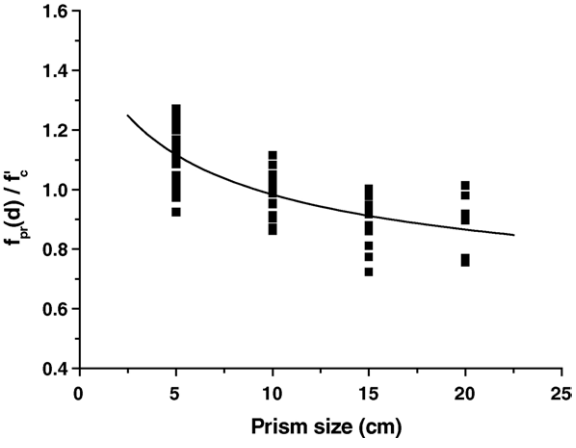

Fig. 3. Size effect for prisms.

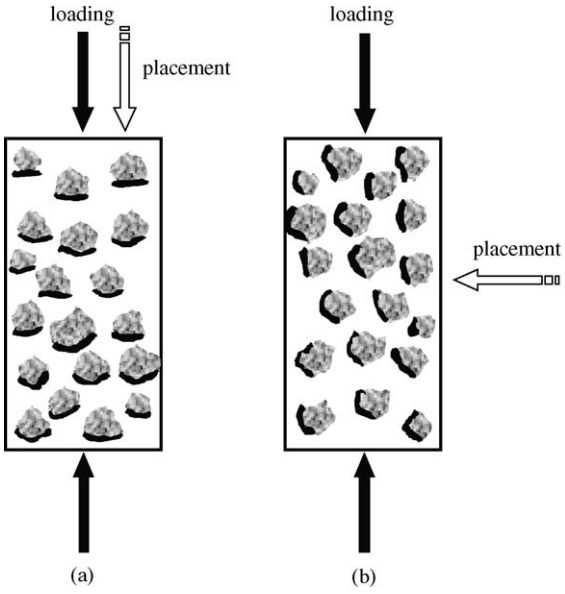

Fig. 4. Illustrations of loading and placement directions.

called the length effect (Kim et al., 2001; Markeset and Hillerborg, 1995; Jansen and Shah, 1997) is present.

4.5. Size effect with placement direction

Fig. 4 indicates illustration of loading direction and placement direction. More specifically, Fig. 4(a) presents the case in which the placement direction is parallel to the loading direction. In this study, the nomenclatures cy, cu,p, and pr,p belong to this case. Meanwhile, Fig. 4(b) shows the case in which the placement direction is normal to the loading direction. The nomenclatures cu and pr correspond to this case.

Eqs. (6) and (7), for cubes and prisms, are obtained from the analyses when the placement direction is parallel to the loading direction.

$$f_{\mathrm{cu,p}}(d) = \frac{1.48 f'_{\mathrm{c}}}{\sqrt{1 + d/2.6}} + 0.56 f'_{\mathrm{c}} \tag{6}$$

$$f_{\mathrm{pr,p}}(d) = \frac{0.94 f'_{\mathrm{c}}}{\sqrt{1 + d/2.6}} + 0.58 f'_{\mathrm{c}} \tag{7}$$

where $f_{\mathrm{cu,p}}(d)$ and $f_{\mathrm{pr,p}}(d)$ are compressive strengths with size of cubes and prisms, respectively, and are in MPa. The smallest size of the cube and the prism d are in cm. The correlation coefficients of Eqs. (6) and (7) are 0.94 and 0.97, respectively.

To evaluate the effect of placement direction on compressive strengths of cubes and prisms, the relationship curve between Eqs. (4) and (6) and the relationship curve between Eqs. (5) and (7) are shown in Fig. 5(a) and (b), respectively. In these figures, the solid rectangular data points and the thick solid line, and the dashed line represent, correspondingly, experimental data of this study, the results from Eqs. (4) and (5), and the results from Eqs. (6) and (7). From these figures, it is noted that, for cubes, size effect difference with placement direction is insignificant. This is because the failure of cubes occurs not due to lateral expansion but due to crushing and the lateral expansion is restrained due to the end restraint occurred by the machine platen.

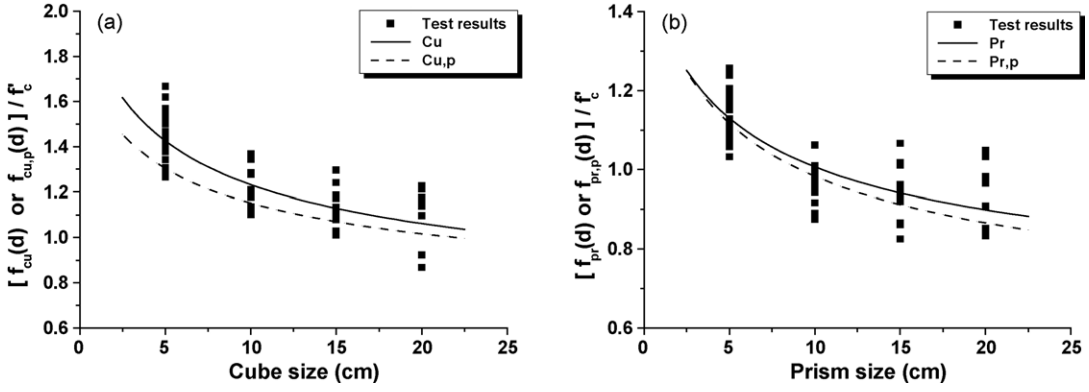

Fig. 5. Size effect with placement direction: (a) cubes; (b) prisms.

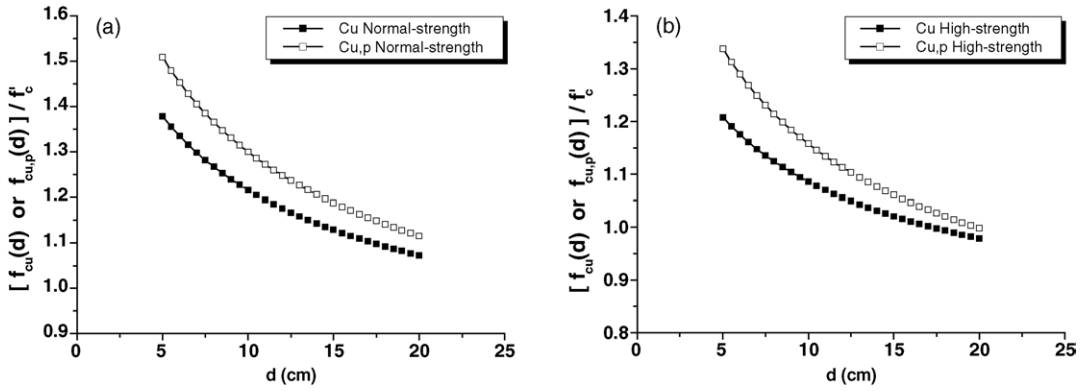

Fig. 6. Effect of placement direction on compressive strength of cubes: (a) normal-strength concrete; (b) high-strength concrete.

When, for prisms, the placement direction is parallel to the loading direction, size effect is more apparent compared to that of the normal case. This is because, when the loading direction is equal to the placement direction, the length effect is additionally imposed on the size effect of the member. In Figs. 5–8, B and α mean the empirical constants of Eq. (1).

4.5.1. Effect of placement direction on compressive strength with strength level

Figs. 6 and 7 show the effect of placement direction on compressive strength with strength level. After the experimental data of cubes and prisms were grouped into NSC and HSC, the analyses were carried out. Where the nomenclatures NSC and HSC are classified based on concrete compressive strengths as follows: NSC of 27.0 and 42.9 MPa; HSC of 65.9 and 78.1 MPa. In Figs. 6 and 7, the solid rectangular data points and the hollow rectangular data points represent, respectively, the results from the normal case and the parallel case.

4.5.1.1. Cubes. From Fig. 6, it is noted that, for cubes, when the placement direction is parallel to the loading direction, the compressive strength is higher than the normal case. For NSC, the size effect difference with displacement direction is not distinct compared to HSC. The reason is that, for NSC, the general fracture mechanism based on the movement of water is changed by the end restraint effect occurred due to the machine platen as well as the failure pattern (in this study, it is a crushing failure).

Meanwhile, for HSC, the difference is more apparent than NSC. This is because, as the strength increases, the size of FPZ decreases and the FPZ of the similar and sufficient size forms in the specimen. Accord-

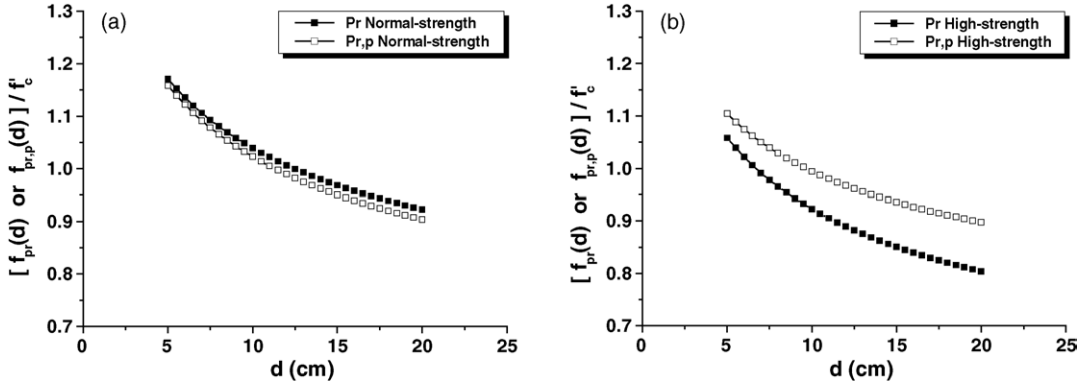

Fig. 7. Effect of placement direction on compressive strength of prisms: (a) normal-strength concrete; (b) high-strength concrete.

ingly, the strengths of both specimens become a similar value. And, when the compressive test for cubes is performed, since the loading direction is normal to the placement direction, nonhomogeneous characteristics occurred due to the settlement difference of materials is additionally reflected on the reduction of the strength. Namely, the size effect of cubes is more apparent compared to cylinders regardless of strength level. This pattern is also similar with contents as illustrated in CEB-FIP Code (1993).

4.5.1.2. Prisms. Chin et al. (1997) evaluated, the stress–strain curve with placement direction using prisms. According to their research results, for NSC, when the placement direction is parallel to the loading direction, insufficient bonding strengths and voids along to the beneath surface of the coarse aggregate occurs. It is due to the differences for the type and content of hydration products formed in concrete, type of aggregate, quantity and quality of interfacial zone formed between the hydrate phase and aggregate, water migration, and etc. Those cannot resist nearly deformations and local shear failures and the failure happens along the surrounding surface of coarse aggregate. Accordingly, the compressive strength of parallel case is smaller than the normal case. For HSC, however, the causes of the fractural mechanism, which occur for NSC, are reduced due to relatively low water-cementitious materials ratio as well as mineral admixture used in concrete production. Accordingly, when the placement direction is parallel to the loading direction, the strength is larger than the normal case.

In this study, the similar conclusion to Chin et al.'s research results (1997) was also drawn. As shown in Fig. 7, for NSC, when the placement direction is parallel to the loading direction, the compressive strength is smaller than the normal case and the difference is insignificant. For HSC, however, the contrary conclusion was found out. The reason is because the fracture mechanism due to various reasons, above-mentioned, occurred for NSC is disappeared for HSC and the influence of unbalance by the segregation difference of the aggregate on the compressive strength becomes more important. In addition, for NSC, the difference of compressive strengths with placement direction is not apparent. For HSC, however, the difference is distinct. From Fig. 7(b), it is noted that, for HSC, when the placement direction is normal to the loading direction, the size effect is more significant than the parallel case.

4.5.2. Effect of strength level on shape effect of compressive strength

Fig. 8 shows the comparison of regression analysis results for cylinders and cubes when the placement direction is normal to the loading direction. After the experimental results were grouped into NSC and HSC, the analyses were performed. In these figures, the solid rectangular data points and the hollow rectangular data points represent, respectively, the results from cubes and cylinders.

The effect of strength level on the shape effect of the compressive strength decreases as the specimen size increases regardless of strength level. More specifically, for HSC, the difference of compressive strengths

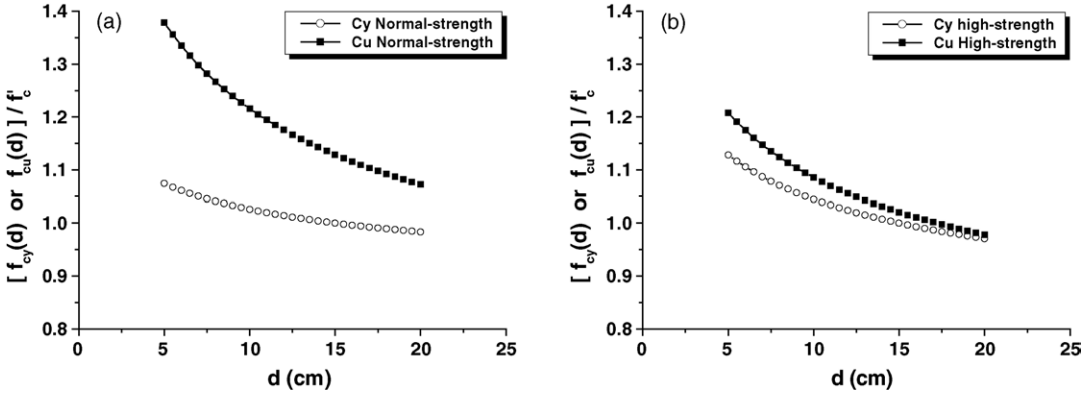

Fig. 8. Effect of strength level on shape effect of compressive strength: (a) normal-strength concrete; (b) high-strength concrete.

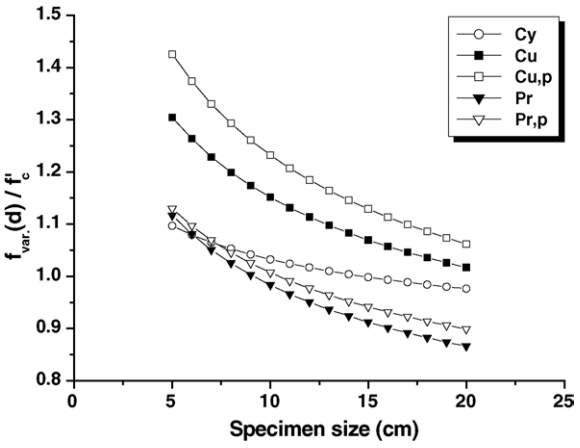

Fig. 9. Relationship between relative strengths and specimen size d.

between cylinders and cubes is more rapidly disappeared than that of NSC. The reason is similar to contents illustrated in Section 4.5.1.1.

4.6. Strength conversions with specimen size and shape

Fig. 9 shows the values of model Eqs. (3)–(7) as a function of the corresponding characteristic dimension d. From this figure, cubes and prisms show more distinct size effect compared with cylinders. More specifically, the effect for prisms is the largest. In addition, for prisms, the difference of compressive strengths with placement direction is smaller than cubes.

Tables 4 and 5 tabulate the conversion factor (CF) calculated using B and α values of Figs. 6–8. Where the basic sizes are Ø100 mm × 200 mm and Ø150 mm × 300 mm cylinders. Based on Fig. 9 and Tables 4 and 5, it is also noted that the compressive strength of the specimen having a general size, shape, and placement direction can transfer to the value corresponding to the specific specimen.

Table 4
Conversion factors with sizes and shapes of the specimen for normal-strength concrete

Cylinder specimen's size and CF	d (mm)	cy	cu	pr	cu,p	pr,p
cy (100), CF = 1.0	50	1.05	1.34	1.14	1.47	1.13
	100	1.00	1.18	1.01	1.27	1.00
	150	0.97	1.10	0.94	1.16	0.93
	200	0.96	1.05	0.90	1.09	0.88
cy (150), CF = 1.0	50	1.07	1.38	1.17	1.51	1.16
	100	1.03	1.22	1.04	1.30	1.02
	150	1.00	1.13	0.97	1.19	0.95
	200	0.98	1.07	0.92	1.12	0.90

Table 5
Conversion factors with sizes and shapes of the specimen for high-strength concrete

Cylinder specimen's size and CF	d (mm)	cy	cu	pr	cu,p	pr,p
cy (100), CF = 1.0	50	1.08	1.16	1.01	1.28	1.06
	100	1.00	1.04	0.88	1.11	0.95
	150	0.96	0.98	0.81	1.02	0.90
	200	0.93	0.94	0.77	0.96	0.86
cy (150), CF = 1.0	50	1.13	1.21	1.06	1.34	1.10
	100	1.04	1.09	0.92	1.16	0.99
	150	1.00	1.02	0.85	1.06	0.94
	200	0.97	0.98	0.80	1.00	0.90

4.7. Relationship between specimen shapes

Fig. 10 shows plots of the cube strength against the cylinder compressive strength for representative specimen sizes. In these figures, solid lines and dashed lines indicate the best-fit lines obtained from the linear regression analyses and the lines of equality $y = x$, respectively. In addition, the equations shown in Fig. 10 are obtained from the linear regression analyses with test data points. The 150 mm cube strength, when plotted against the corresponding Ø150 mm × 300 mm cylinder strength as shown in Fig. 10(a), shows that cube strength is higher for lower grades of concrete. At approximately 65 MPa, however, the two strengths become identical. After that point, standard cylinders indicate a slightly higher strength than that of the corresponding cubes. As shown in Fig. 10(b) and (c), the slope of the best-fit lines is not rapider than that of Fig. 10(a). However, it is noted that it displays a similar trend with Fig. 10(a). In Fig. 10(d), the similar observations may also be noted from Fig. 10(a). At approximately 60 MPa, the two strengths become identical.

Meanwhile, the relationship between prisms and cylinders can be analogized from some literatures. Namely, Markeset (1995) and Markeset and Hillerborg (1995) experimentally showed that the post-peak energy per unit area is independent of the spec-

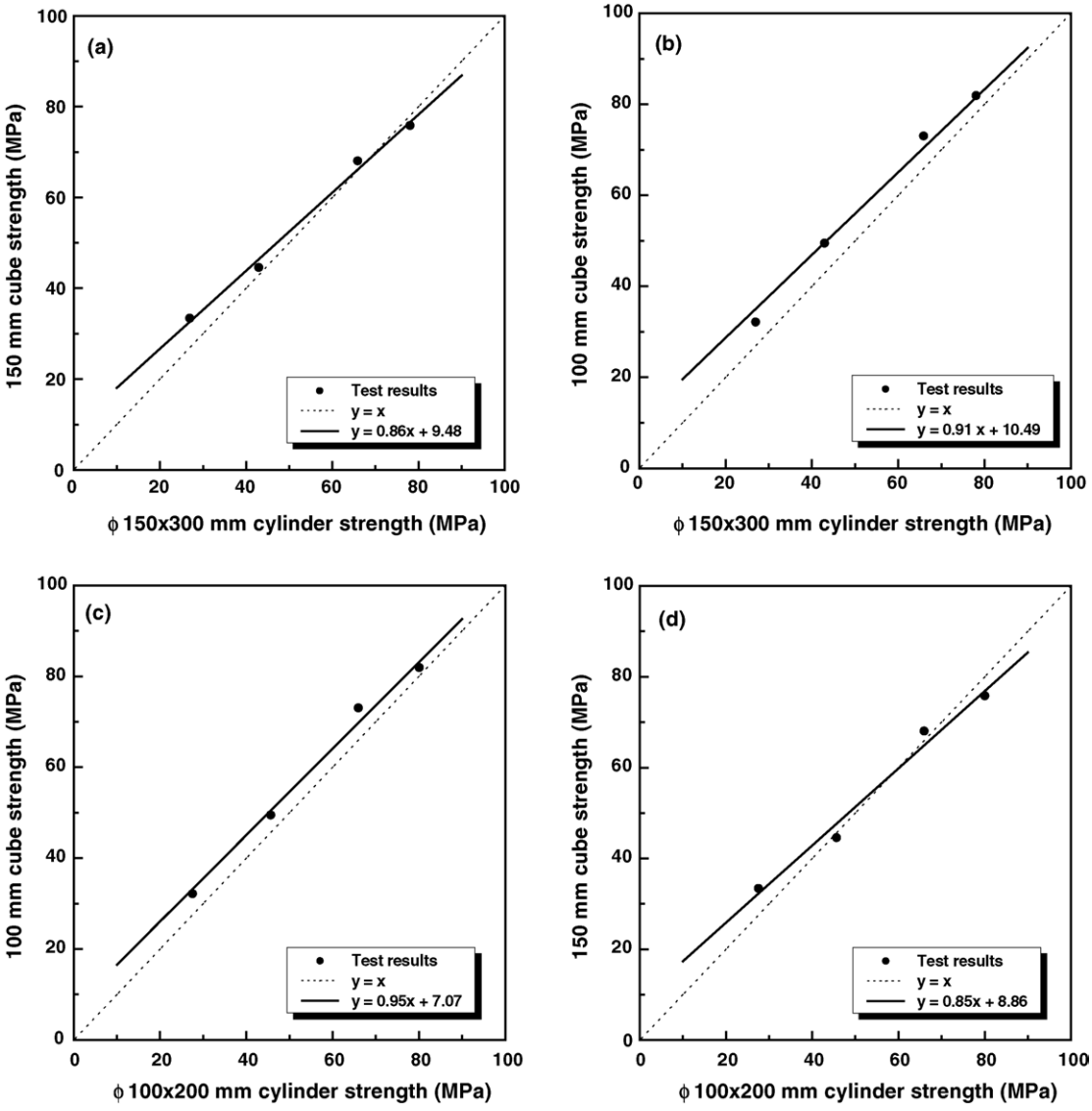

Fig. 10. (a) Relationship between compressive strengths of 150 mm cube and Ø150 mm × 300 mm cylinder; (b) relationship between compressive strengths of 100 mm cube and Ø150 mm × 300 mm cylinder; (c) relationship between compressive strengths of 100 mm cube and Ø100 mm × 200 mm cylinder; (d) relationship between compressive strengths of 150 mm cube and Ø100 mm × 200 mm cylinder.

imen length when the slenderness is greater than approximately 2.50 for concrete cylinders. Jansen and Shah (1997) also experimentally showed that pre-peak energy per unit cross-sectional area increases proportionally with specimen length and post-peak energy per unit cross-sectional area does not change with specimen length for lengths greater than 20.0 cm in concrete cylinders. Kim et al. (2001) concluded that flexural compressive strength does not change for specimens having a length greater than 30.0 cm for C-shaped concrete specimens having a rectangular cross-section. From these contents, we can conclude that the relationship between prisms and cylinders will be similar with the relationship between cubes and cylinders.

4.8. Generalization of strength prediction equations for cubes and prisms

To obtain the concrete compressive strength for cylinders, to know a model equation commonly applicable to both specimen shapes (i.e. (1) cylinders and cubes and (2) cylinders and prisms) is very useful. Fig. 11(a) and (b) shows the relationship between strengths of cube and cylinder and the relationship between strengths of prism and cylinder, respectively. In these figures, solid lines and dashed lines indicate the best-fit lines obtained from the linear regression analyses and the lines of equality $y = x$, respectively. Accordingly, when designers or contractors know the cube or prism strength, it is possible to obtain the strength of cylinder corresponding to the cube or prism based on the equations shown in Fig. 11.

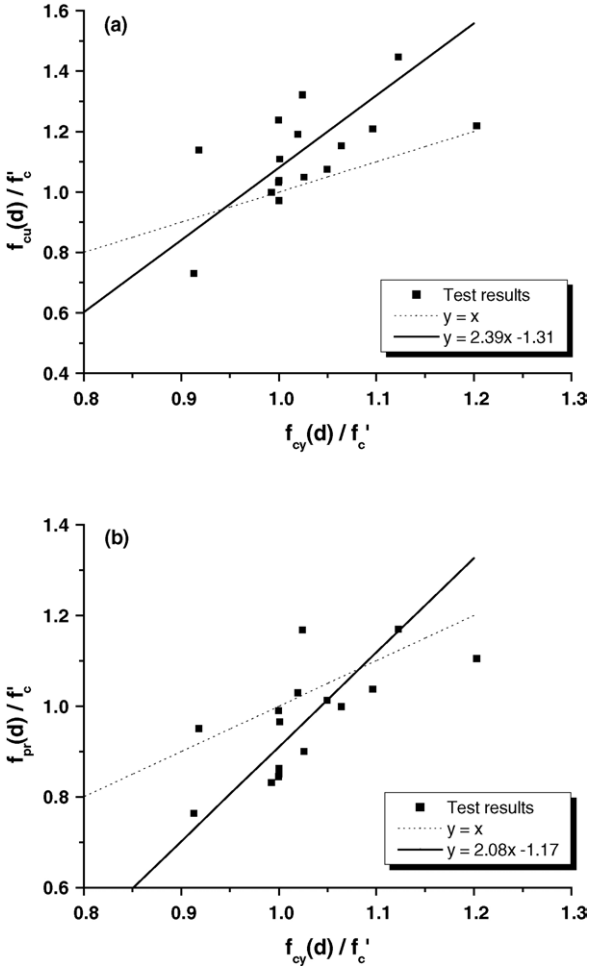

Fig. 11. Generalization of strength prediction equations for cubes and prisms: (a) relationship between strengths of cube and cylinder; (b) relationship between strengths of prism and cylinder.

5. Summary and conclusions

The following conclusions are applicable to the particular test materials and test procedures employed.

1. Size effect based on the specimen size and shape difference is present. The size effect for cubes and prisms is stronger than cylinders.
2. To obtain the concrete compressive strength, model equations applicable to cylinders, cubes, and prisms are suggested. In addition, correlations between compressive strengths with size, shape, and placement direction of the specimen are investigated. Additionally, to obtain the concrete compressive strength of cylinder from other specimen shapes, model equations commonly applicable to both specimen shapes (i.e. (1) cylinders and cubes and (2) cylinders and prisms) are suggested.
3. For the effect of placement direction on the compressive strength, cubes made of NSC do not show a distinct influence. For HSC, however, the difference is apparent. For prisms made of NSC, when the placement direction is parallel to the loading direction, the compressive strength is smaller than the normal case. For HSC, however, the contrary conclusion was found out.
4. Effect of strength level on the shape effect of compressive strengths decreases as the specimen size increases. More specifically, for HSC, the difference of compressive strengths between cylinders and cubes is more rapidly disappeared than that of NSC.
5. The results suggest that the current strength criteria based design practice should be revised. In designing concrete structures, it is more desirable to use the compressive strength of concrete obtained not from standardized specimens such as Ø150 mm × 300 mm or Ø100 mm × 200 mm cylinders but from specimens based on size, shape, and placement direction of actual structures.

6. Validity limits

Since this experimental study was done for given vibration and curing conditions (see Section 3.1) with the given mixture compositions (see Table 1) and for given four w/c ratios (28, 35, 50, and 67%), further experimental work involving variances at each test variables would be required for more broad generalization.

Acknowledgements

This work was supported by Korea Research Foundation Grant (KRF-2003-003-D00324). The authors would like to deeply thank the foundation for financial support. This support is deeply appreciated.

References

ASTM Standards, 1999. Standard test method for obtaining and testing drilled cores and sawed beams of concrete. In: Annual Book of ASTM Standards (ASTM C 42-99). American Society for Testing and Materials, Philadelphia, 4 pp.

ASTM Standards, 2001. Standard test method for compressive strength of cylindrical concrete specimens. In: Annual Book of ASTM Standards (ASTM C 39-01). American Society for Testing and Materials, Philadelphia, 5 pp.

Bazant, Z.P., 1984. Size effect in blunt fracture; concrete, rock, metal. J. Eng. Mech. ASCE 110 (4), 518–535.

Bazant, Z.P., 1987. Fracture energy of heterogeneous material and similitude. In: SEM-RILEM International Conference on Fracture of Concrete and Rock, pp. 390–402.

Bazant, Z.P., 1993. Size effect in tensile and compressive quasibrittle failures. In: JCI International Workshop on Size Effect in Concrete Structures, pp. 141–160.

Bazant, Z.P., Xiang, Y., 1997. Size effect in compression fracture: splitting crack band propagation. J. Eng. Mech. ASCE 123 (2), 162–172.

Benjamin, J.R., Cornell, C.A., 1970. Probability, Statistics, and Decision for Civil Engineers. McGraw-Hill Publishing Company, New York (Section 4.3).

CEB-FIP Model Code, 1990, 1993. Comite Euro-International du Beton (CEB), Bulletin D'Information No. 203/205, Lausanne, 437 pp.

Chin, M.S., Mansur, M.A., Wee, T.H., 1997. Effects of shape, size, and casting direction of specimens on stress–strain curves of high-strength concrete. ACI Mater. J. 94 (3), 209–219.

Gonnerman, H.F., 1925. Effect of size and shape of test specimen on compressive strength of concrete. ASTM Proc. 25, 237–250.

Gyengo, T., 1938. Effect of type of test specimen and gradation of aggregate on compressive strength of concrete. J. ACI 33, 269–283.

IMSL, 2003. Library, 8th ed. IMSL, Inc.

Jansen, D.C., Shah, S.P., 1997. Effect of length on compressive strain softening of concrete. J. Eng. Mech. ASCE 123 (1), 25–35.

Kim, J.H.J., Yi, S.T., Kim, J.K., 2004. Size effect of concrete members applied with flexural compressive stresses. Int. J. Fracture 126 (1), 79–102.

Kim, J.K., Eo, S.H., 1990. Size effect in concrete specimens with dissimilar initial cracks. Mag. Concrete Res. 42 (153), 233–238.

Kim, J.K., Kim, M.S., Yi, S.T., Kim, J.H.J., 2005. Size effect on flexural compressive strength of reinforced concrete beam members. Mag. Concrete Res., submitted for publication.

Kim, J.K., Yi, S.T., Kim, J.H.J., 2001. Effect of specimen sizes on flexural compressive strength of concrete. ACI Struct. J. 98 (3), 416–424.

Kim, J.K., Yi, S.T., Park, C.K., Eo, S.H., 1999. Size effect on compressive strength of plain and spirally reinforced concrete cylinders. ACI Struct. J. 96 (1), 88–94.

Kim, J.K., Yi, S.T., Yang, E.I., 2000. Size effect on flexural compressive strength of concrete specimens. ACI Struct. J. 97 (2), 291–296.

Mansur, M.A., Islam, M.M., 2002. Interpretation of concrete strength for nonstandard specimens. J. Mater. Civil Eng. ASCE 14 (2), 151–155.

Markeset, G., Hillerborg, A., 1995. Softening of concrete in compression localization and size effects. Cement Concrete Res. 25 (4), 702–708.

Markeset, G., 1995. A compressive softening model for concrete. In: Wittmann, F.H. (Ed.), Fracture Mechanics of Concrete Structures, FRAMCOS-2, AEDIFICATIO Publishers, pp. 435–443.

Murdock, J.W., Kesler, C.E., 1957. Effect of length to diameter ratio of specimen on the apparent compressive strength of concrete. ASTM Bull. 221, 68–73.

Yi, S.T., Kim, J.H.J., Kim, J.K., 2002. Effect of specimen sizes on ACI rectangular stress block for concrete flexural members. ACI Struct. J. 99 (5), 701–708.